A unified approach to parametric geocoding and atmospheric/topographic correction for wide field-of-view airborne imagery
Part 2: atmospheric / topographic correction

Rudolf Richter
DLR - German Aerospace Center
Remote Sensing Data Center
D - 82234 Wessling / Germany

Daniel Schläpfer
University of Zurich
Remote Sensing Laboratories (RSL)
Winterthurerstr. 190
CH-8057 Zurich / Switzerland

Abstract

A method for the radiometric correction of wide field-of-view airborne imagery has been developed that accounts for the angular dependence of the path radiance and atmospheric transmittance functions to remove atmospheric and topographic effects. The first part of processing is the parametric geocoding of the scene to obtain a geocoded, orthorectified image and the view geometry (scan and azimuth angles) for each pixel as described in part 1 of the jointly submitted paper.
The second part performs the combined atmospheric/topographic correction and consists of three steps. The first step of the algorithm employs a radiative transfer code to calculate look-up tables of the atmospheric correction functions (path radiance, atmospheric transmittance, direct and diffuse solar flux) that depend on scan angle, relative azimuth angle between scan line and solar azimuth, and terrain elevation. For repeated later use, results can be stored in a spectral database for the solar (0.35-2.55 µm) and thermal region (8-14 µm). The second step performs the resampling with the channel-specific spectral response of the sensor. The third step calculates surface reflectance (0.35-2.55 µm) and surface temperature (8-14 µm) using the information of a digital terrain model to account for surface elevation, slope, and orientation.
The issues of the database size and accuracy requirements are critically discussed. The method supports all common types of imaging airborne optical instruments: panchromatic, multispectral, and hyperspectral, including fore/aft tilt sensors. An example of processing of hyperspectral imagery in rugged terrain is presented and discussed.

1. Introduction

The objective of any radiometric correction of airborne and spaceborne land imagery of optical sensors is the extraction of physical earth surface parameters such as reflectance and temperature. To achieve this goal the influence of the atmosphere, solar illumination, sensor viewing geometry, and terrain information have to be taken into account. A number of papers have been published recently presenting physically-based models for the combined correction of atmospheric/topographic effects (Sandmeier and Itten 1997, Staenz and Williams 1997, Richter 1998). Most of the models are restricted to narrow field-of-view sensors, because the scan angle dependence of the atmospheric path radiance and transmittance functions is neglected. This contribution includes a full treatment of atmospheric scan angle effects, includes a processing of thermal bands to derive surface temperature, and has an interface to surface energy-balance models.

2. Atmospheric and Topographic Correction Model (ATCOR4)

The radiometric correction is based on the geocoded, orthorectified image as described in part 1 of this paper. Part 2 of the processing requires the generation of the atmospheric look-up tables pertaining to the image (flight and solar geometry, range of ground elevations, atmospheric parameters such as aerosol type and optical depth, water vapour, and ozone content) if not existing in the database, and the resampling with the spectral response channels of the sensor, see figure 1. The image-based atmospheric / topographic correction is performed iteratively (Richter 1998, 2000). Initially, the scene is treated as consisting of Lambertian (isotropically reflecting) surface elements. This is a fairly good approximation for near-nadir viewing geometries (scan angle < 10°) when the solar backscatter region is avoided. However, many surface covers show anisotropic reflectance behaviour, especially over the large range of view angles that are typically encountered for airborne scanners (30-90° field-of-view). Unfortunately, there is no generally applicable model to account for BRDF (bidirectional reflectance distribution function) effects over land, where a large variety of surface covers exists. Therefore, an interface to scene-dependent models is provided that can be adapted interactively to deal with BRDF effects, see section 2.2.
In those cases where airborne scenes are available only for one flightline the restricted number of view angles and the fixed solar geometry do not allow the retrieval of bidirectional parameters and one has to use the Lambertian assumption. Usually, there is also no bidirectional reflectance information available from other sources at the typical 1-10 m scale of airborne imagery.
The ATCOR4 model presented here is an extension of the ATCOR3 model (Richter 1998). Similar to other authors (Staenz and Williams 1997) a look-up table (LUT) approach is used for the atmospheric correction employing the Lambertian assumption, since bidirectional surface reflectance models would result in prohibitively large atmospheric databases. The model consists of the following major modules :

- Module ATLUT calculates scan angle and elevation dependent atmospheric LUT‘s employing the radiative transfer code MODTRAN4 (Berk et al. 1998). ATLUT submits all MODTRAN runs according to user specifications and condenses the MODTRAN output files (called “*.tp7“) into much smaller spectral files (called “*.sp7“) containing the required minimum spectral information. All condensed “*.sp7“ files can be put into a permanent spectral atmospheric database. The size is currently about 2 Gigabytes, about a factor 5 smaller than the corresponding “*.tp7“ database would be.
- Module RESLUT resamples the spectral LUT “*.sp7“ with the band-specific response functions of the selected sensor.
- Module ATCOR4 performs the combined atmospheric / topographic correction accounting for the angular and elevation dependence of the atmospheric correction functions and calculates surface reflectance (solar spectral region) and surface temperature (thermal region) based on the geocoded or orthorectified imagery. The special case of a flat terrain is also included.

2.1 Considerations for the atmospheric database

The main design drivers of modules ATLUT and RESLUT are the size and the accuracy of the spectral database for the atmospheric correction and the appropriate selection of the options for the radiative transfer (RT) calculations to minimize the computing time without sacrificing the accuracy. The size of the ATLUT output files is minimized compared to the standard MODTRAN output by including only the required information in the compressed files, i.e., spectral path radiance, direct and diffuse transmittance, direct and diffuse flux, and spherical albedo. Further considerations are the selection of the scan angle increment to keep interpolation errors small, the spectral resolution, and the number of streams for the multiple scattering calculations. These items are discussed now. More details are given elsewhere (Richter 2000). The

advantage of the database is the possible repeated use of the results of radiative transfer calculations requiring only a resampling with the sensor-specific response functions.

- For the solar region, MODTRAN's DISORT option (discrete ordinate radiative transfer, Stamnes et al. 1988) with 8 streams is used as default at a spectral resolution of 15 cm^{-1} . Tests were run with 16 streams also, but results were close to the 8-stream results for scan angles smaller than 60° and solar zenith angles smaller than 70°. However, Isaacs 2-stream option can also be selected by the user for a faster, but less accurate, processing. The spectral resolution is selected at 15 cm^{-1} in the wavelength range 0.35-1.8 µm. A 1 cm^{-1} grid averaged to 4 cm^{-1} is employed in the 1.8 – 2.55 µm range to improve the spectral resolution to about 2 nm in the short-wave region.
- In the thermal region a 2-stream RT calculation is sufficient. Here, the highest spectral resolution of MODTRAN (1 cm^{-1}) is employed, which is equivalent to a 10 nm resolution at the wavelength 10 µm.
- Calculations intended for permanent use in the database are performed for a large swath angle (typically ±40° with respect to nadir) comprising the spectral regions 0.35-2.55 µm and 8-14 µm. The scan angle range and spectral regions cover the need for most earth observing multispectral / hyperspectral sensors (Vane et al. 1993, Cocks et al. 1998, Strobl et al. 1996, Gower et al. 1992). The 3-5 µm atmospheric window region is currently not included, because the separation of reflected solar and emitted thermal radiation is difficult, especially with a small number of channels.
- The scan angle increment should be large on the one hand to reduce the number of RT calculations, but it should be small to keep any scan angle interpolation errors small. As a compromise, the recommended scan angle increment is carefully selected at 5° to keep the relative interpolation error in the at-sensor radiance smaller than 1 % for scan angles up to 40°. However, calculations can also be defined for a smaller swath angle, e.g. 10°, to reduce the time for the LUT calculation. For cases where a digital elevation model is employed the elevation range (minimum, maximum) and elevation increment have to be specified by the user. RT calculations are then performed for the discrete set of selected elevations and scan angles.

2.2 Interface to BRDF models

It is well known that many surface covers show BRDF effects (Kriebel 1978), however, there is no generally applicable model for all land scenarios. Most BRDF models are empirical or semi-empirical models where three or four parameters have to be fitted depending on surface cover, available view and illumination geometries (Roujean et al. 1992, Wu et al. 1995) and physical parameters (leaf are index or vegetation index).
Thus, specialized scene-specific evaluations are possible depending on the available number of solar and viewing geometries. Therefore, an interface to BRDF models is included. ATCOR4 first performs the atmospheric/topographic correction based on the assumption of Lambertian surface elements. Then, the SPECL program performs a spectral preclassification of the reflectance cube and returns a map of class indices for each pixel. If the spectral signature agrees within certain margins with one of the class template spectra it is put into this class, otherwise it belongs to the class *undefined* (see Richter 2000 for details). For each pixel of a certain class i the viewing and solar geometry is known, and depending on the available range of angles a 3- or 4-parameter fit can be tried with a user-defined BRDF model. The user has access to the class map, the reflectance cube(s), DEM files (elevation, slope, aspect) and to the view angle file from PARGE (scan and azimuth angle for each pixel).

3. Example of processing: DAIS-7915 imagery of Timna, Israel

As a sample case of processing in rugged terrain a subimage of a DAIS-7915 scene of Timna (Israel) is taken. The DAIS sensor records imagery in 79 channels from the visible (0.5 µm) to the thermal (13 µm) spectrum with a 52° field-of-view. Details concerning the instrument are given elsewhere (Strobl et al. 1996). The geographic coordinates of the area are: longitude 34.9°, latitude 29.8°. The complete scene of flightline 1 (Timna north) comprises about 3000 scan lines and was acquired on 31 July 1997 at 9:33-9:37 h local time. The flight altitude was 3650 m above sea level, the heading was 156°. The solar zenith and azimuth angles were 31.7° and 104.0°, respectively.
The image was processed in the framework of a project of the German-Israeli Foundation. A digital elevation model of resolution 25 m (Hall 1996) was resampled to 5 m using bilinear interpolation to fit the ground sampling distance of the DAIS sensor. The mosaicked image of figure 1 shows the DEM and related information (slope, aspect, sky view factor, solar illumination). As a first processing step the parametric geocoding software PARGE (Schläpfer et al. 1998, and this issue) was used to calculate the orthorectified imagery. Information concerning the angular movements of the platform was taken from the DAIS gyros (roll, pitch, yaw), GPS position data was recorded with a NovAtel system (NovAtel Communications Ltd 1994). The information concerning the scan and azimuth angles for each pixel is calculated and stored in a PARGE / ATCOR4 interface file. So, the complete viewing and solar illumination geometry is known for each image pixel. Due to some GPS problems the accuracy of the orthorectification is approximately 3-8 pixels.

Figure 2 shows the results of the combined atmospheric / topographic correction. In many cases the spatial resolution of the available DEM is not adequate to the sensor's pixel size, and this situation also exists here. So, regions of steep slopes and rapid slope or aspect changes are not adequately represented in the interpolated DEM. Large radiometric errors (over- or under-correction) can therefore be expected in those regions (Richter 1998). However, high spatial resolution DEMs of 1 – 5 m for airborne imagery are very expensive and often not available as in this case. So, one has to make a compromise. An additional error source is the accuracy of the orthorectification. Nevertheless, for most regions of the image the topographic illumination influence is clearly reduced. Figure 3 demonstrates the reversal of brightness values in the spectral domain that is caused by the topographic effect: if a pixel is oriented towards the sun, the surface appears bright, and the reflectance spectrum without consideration of the topography (dashed line) lies above the spectrum that accounts for topography. If a pixel is oriented away from the sun, the surface appears darker. Therefore, the reflectance spectrum without consideration of the topography (dashed line) lies below the spectrum that accounts for topography.

4. Conclusions

A unified approach to parametric geocoding and atmospheric / topographic correction for airborne imagery has been developed. The model supports the geometries of most current airborne instruments including along-track (fore/aft) viewing sensors. Panchromatic, multispectral, and hyperspectral imagery from the solar spectral region and thermal region can be processed to obtain surface reflectance and temperature images. A large database may be used to avoid time-consuming runs with a radiative transfer code for cases that are already included in the database. Only a resampling with the channel-specific spectral response of the selected instrument is required in these cases before processing the image data.
The method was successfully employed for the HyMap and DAIS-7915 hyperspectral sensors in the framework of airborne ESA and national campaigns in 1998/1999. Good agreement of derived spectra (0.01-0.02 reflectance units) was obtained with simultaneous ground reflectance measurements in the near-nadir range and in flat terrain. For off-nadir angles larger than 10° bidirectional reflectance effects can play a role, leading to deviations from the nadir

reflectance values. Therefore, a BRDF interface has been provided to enable application-dependent corrections. For imagery in mountainous terrain the topographic illumination effect is strongly reduced by the proposed radiometric method even if the spatial resolution of a DEM is often not sufficient and one has to compromise.

References

Berk, A., et al., 1998, S. M., MODTRAN cloud and multiple scattering upgrades with application to AVIRIS, *Remote Sensing of Environment* **65**, 367-375.

Cocks, T., et al. 1998, The HyMap airborne hyperspectral sensor: the system, calibration and performance, *First EARSeL Workshop on Imaging Spectroscopy, 6-8 Oct. 1998, Zurich, Switzerland*, pp. 37-42.

Gower, J. F. R. et al. 1992, CCD-based imaging spectroscopy for remote sensing: the FLI and CASI programs, *Canadian J. Remote Sensing* **18**, 199-208.

Hall, J. K., 1996, Digital topography and bathymetry of the area of the Dead Sea depression, *Tectonophysics* **266**, 177-185.

Kriebel, K. T., 1978, Measured spectral bidirectional reflection properties of four vegetated surfaces, *Applied Optics* **17**, 253-259.

NovAtel Communications Ltd, 1994, GPSCard™ Command Descriptions Manual, Calgary, Alberta, Canada.

Richter, R., 1998, Correction of satellite imagery over mountainous terrain, *Applied Optics* **37**, 4004-4015.

Richter, R., 2000, Model ATCOR4: Atmospheric / topographic correction for wide FOV airborne imagery, report DLR-IB 564-04/00, Wessling, Germany.

Roujean, J. L., et al. 1992, A bidirectional reflectance model of the earth's surface for the correction of remote sensing data, *J. Geophys. Research*, **97**, 20 455-20468.

Sandmeier, S., and Itten, K. I., 1997, A physically-based model to correct atmospheric and illumination effects in optical satellite data of rugged terrain, *IEEE Trans. Geosc. Remote Sens.* **35**, 708-717.

Schläpfer, D., Schaepman, M., and Itten, K. I., 1998, PARGE: parametric geocoding based on GCP-calibrated auxiliary data, *SPIE Vol. 3438*, pp. 334-344, San Diego.

Stamnes, K., et al. 1988., Numerically stable algorithm for discrete-ordinate-method radiative transfer in multiple scattering and emitting layered media, *Applied Optics* **27**, 2502-2509.

Strobl, P., et al., 1996, Preprocessing for the Digital Airborne Imaging Spectrometer DAIS 7915, SPIE Vol. **2758**, pp. 375-382, Orlando.

Staenz, K., and Williams, D. J., 1997, Retrieval of surface reflectance from hyperspectral data using a look-up table approach, *Canadian J. Remote Sensing* **23**, 354-368.

Vane, G., et al., 1993, The airborne visible/infrared imaging spectrometer (AVIRIS), *Remote Sensing of Environment*, **44**, 127-143.

Wu, A., Li, Z., and Cihlar, J., 1995, Effects of land cover type and greenness on advanced very high resolution radiometer bidirectional reflectances: analysis and removal, *J. Geophysical Research* **100** 9179-9192.

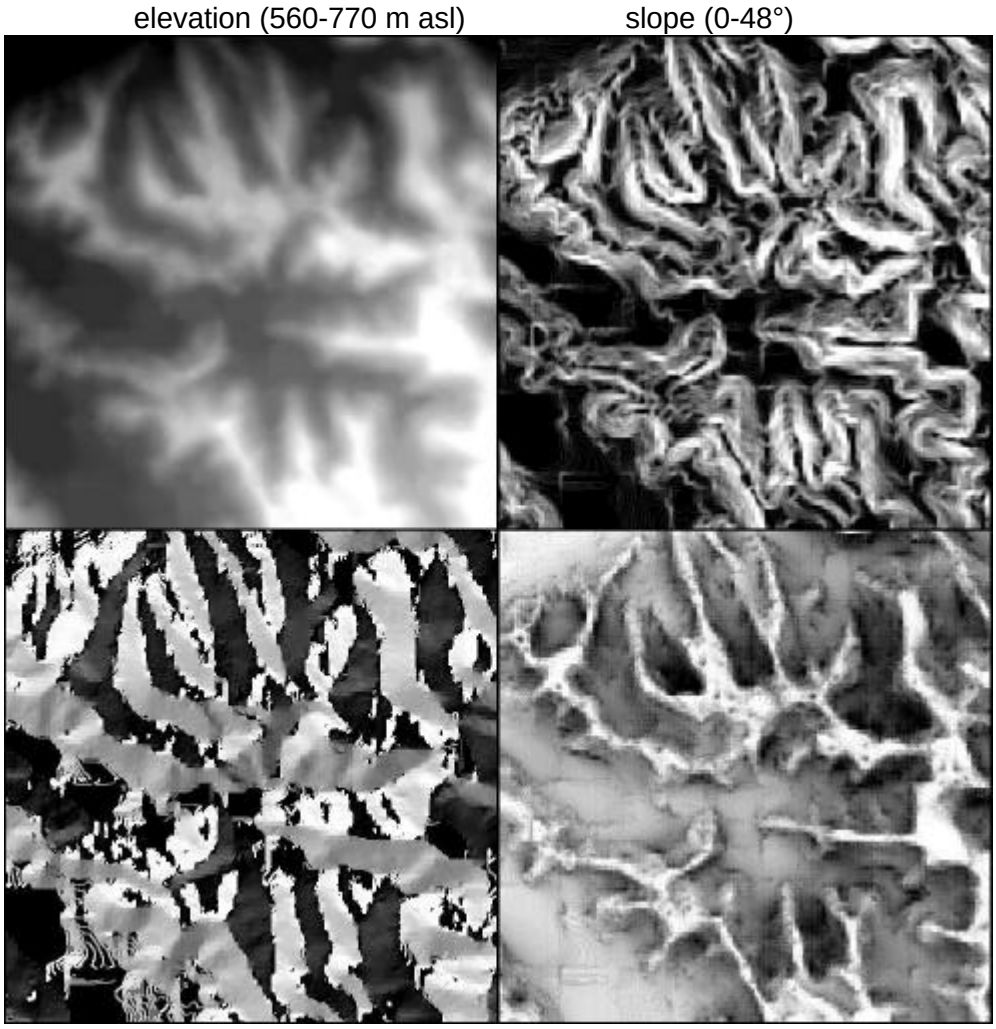

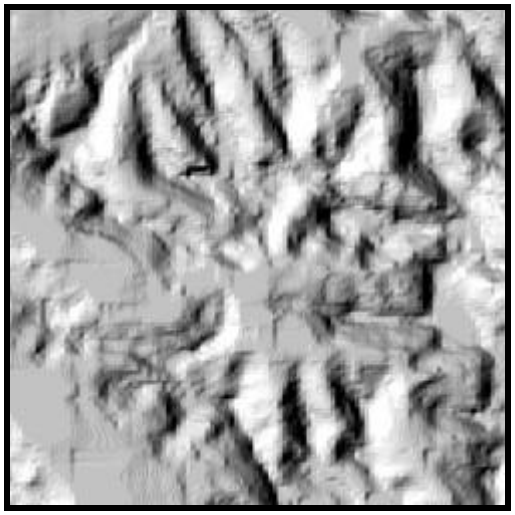

cos β of local solar illumination

Figure 1. Mosaic of DEM related information.

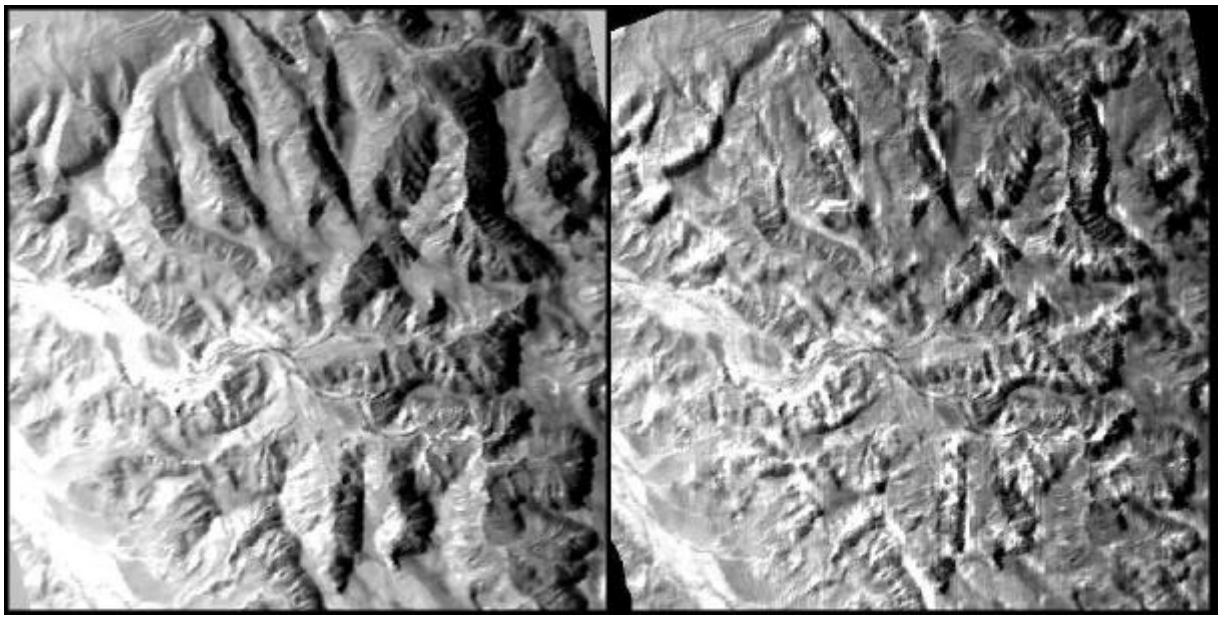

Figure 2. Left: original DAIS imagery; right: after atmospheric / topographic correction. The image shows band 22 (860 nm) of DAIS.

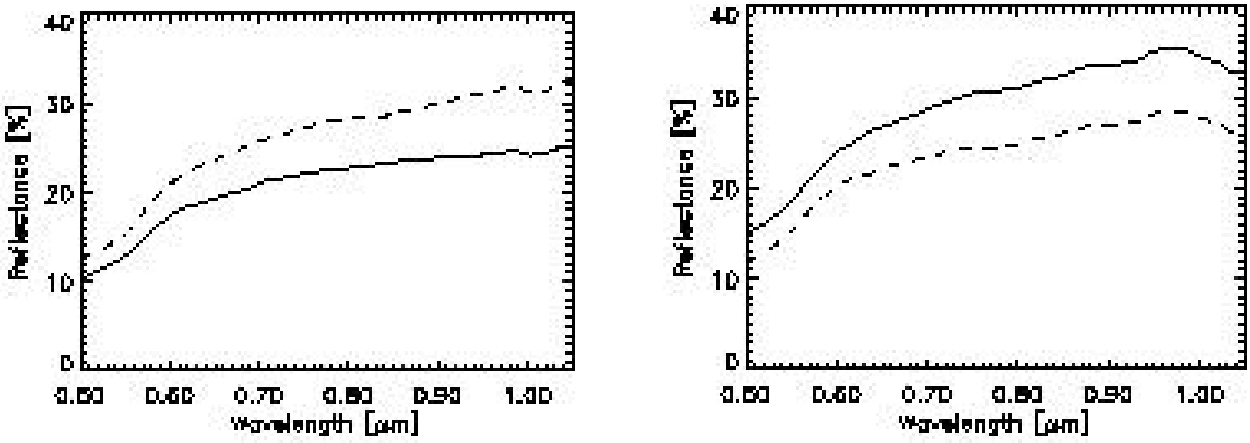

Figure 3. Left: pixel oriented towards the Sun (slope 33°, aspect 143°, illumination angle 21°). Right: pixel oriented away from Sun (slope 39°, aspect 214°, illumination angle 56°). Solid line: atmospheric/ topographic correction, dashed line: only atmospheric correction.